International Journal of Thermophysics, Vol. 22, No. 4, 2001

Complex Formation of Chitosan with Iodine and Its Structure and Spectroscopic Properties—Molecular Assembly and Thermal Hysteresis Behavior[1]

H. Yajima,[2,3] M. Morita,[4] M. Hashimoto,[5] H. Sashiwa,[6] T. Kikuchi,[7] and T. Ishii[2]

To elucidate the factors responsible for the complexation of chitosan with iodine and to gain insight into the structures and spectroscopic properties of chitosan-iodine (CI) complexes, extensive studies were performed on the effects of iodine/chitosan concentrations and temperature on CI complexation and its physicochemical properties in acidic solutions containing excess KI by means of various spectroscopic (absorption, CD, etc.) and structural-analysis (SAXS, etc.) measurements and molecular dynamics (MD) simulations. The CI complex exhibited absorption spectra with a peak at around 500 nm, regardless of the iodine/chitosan concentrations and temperature. Correspondingly, the CI complexes exhibited mutually split CD bands with opposite signs (+, −) at around 500 nm. The CI complex showed thermal hysteresis, i.e., an irreversible reaction process involved in complexation and color formation. Resonance Raman spectra measurements revealed that the iodine species responsible for the purple coloring of the complexes is primarily I_3^- ions. Moreover, ^{13}C-NMR spectra measurements inferred that the interaction sites in the D-glucosamine moiety in chitosan chains with bound iodine are the hydroxyl groups on C-1, C-3, and C-4.

[1] Paper presented at the Fourteenth Symposium on Thermophysical Properties, June 25–30, 2000, Boulder, Colorado, U.S.A.

[2] Department of Applied Chemistry, Faculty of Science, Science University of Tokyo, 1-3 Kagurazaka, Shinjuku-ku, Tokyo 162-8601, Japan.

[3] To whom correspondence should be addressed. E-mail: hyajima@ch.kagu.sut.ac.jp

[4] Design Department, Science Instruments Division, Hitachi Koki Co., Ltd., 1-24-12, Nishi-Shinbashi Minato-ku, Tokyo 105-8717, Japan.

[5] Georemediation Engineering Department, Plant Division, Kurita Water Industries Ltd., 4-7, Nishi-Shinjuku 3-Chome, Shinjuku-Ku, Tokyo 160-8383, Japan.

[6] Functional Polymer Section, Department of Organic Materials, Osaka National Research Institute, 1-8-31 Midorigaoka, Ikeda, Osaka 563-8577, Japan.

[7] Department of Chemical Technology, College of Science and Industrial Technology, Kurashiki University of Science and the Arts, 2640 Nishinoura, Tsurajima-cho, Kurashiki, Okayama 712-8505, Japan.

0195-928X/01/0700-1265$19.50/0

Structural studies based on analytical ultracentrifugation, and SAXS and SANS measurements indicated that the molecular assembly of extended chitosan chains plays a vital role in CI complexation. MD calculations predicted that the irreversibility and thermal hysteresis behavior of the CI complexes are due to a crystalline-like extended → compact folded conformational transition.

KEY WORDS: chitosan-iodine complex; molecular assembly; molecular simulation; physicochemical properties; structural analysis; thermal hysteresis behavior.

1. INTRODUCTION

Chitosan, a linear polysaccharide of β-(1, 4) linked D-glucosamine, obtained primarily as a by-product of the seafood industry, has recently attracted a great deal of attention as a multifunctional biopolymer for industrial, agricultural, medical, and pharmaceutical applications because of its unique properties including a variety of biological activities, biodegradability, biocompatibility, its behavior as a polyelectrolyte, metal-chelating function, flocculation, etc. [1–4]. Chitosan is an acid-soluble and N-deacetylated derivative of chitin, which is widely distributed in nature in bacterial cell walls and in the exoskeletons of crustaceans and insects [1]. For improvement and further development of the potential applications of chitosan, it is necessary to obtain detailed information on its molecular characteristics based on extensive physicochemical studies.

The chain conformations of chitosan molecules in the solid state in the free anhydrous chitosans, acid salts, and transition metal complexes have been studied by various structural analysis techniques such as X-ray diffraction [5–8] and solid-state ^{13}C NMR [9]. Chitosan chains have been reported to assume an extended two-fold helical conformation stabilized by the O3 $\cdots$ O5 hydrogen bond or an extended left-handed 8/5 helical conformation (a relaxed version of the two-fold helix). In addition, X-ray diffraction studies of the molecular and crystal structure of hydrated chitosan by Okuyama et al. [10] revealed that chitosan in the hydrated form assumes a two-fold helix chain conformation, similar to that in the anhydrate, and that water molecules contribute to stabilization of the structure by forming water bridges between polymer chains. On the other hand, a number of studies on the solution properties of chitosan molecules have also been performed by means of various techniques such as viscosity measurement [11–14], static and dynamic light scattering [11, 14, 15], NMR [16], and the Monte Carlo calculation [17]. The characteristics of chitosan are dependent on the degree of deacetylation (DDA), the distribution of acetyl groups, chain length, and molecular weight distribution. Chitosans with different DDAs under different solution conditions (different ionic strength,

pH, or temperature) are predicted to be rod-shaped or a stiff coil [12–14, 17], a random coil [12–14, 18], or a compacted sphere [19] depending on the variables.

Chitosan has been shown to form a colored complex with iodine as seen in the blue iodine complexes of amylose [20–22] and poly(vinyl alcohol) [23, 24]. This reaction has been used for the chitosan test [25–27]. Shigeno et al. [28, 29] studied the adsorption behavior of iodine on chitosan films by physicochemical methods. They reported that iodine adsorption was caused by the formation of charge-transfer complexes between the amino groups of chitosan and iodine molecules. Recent X-ray structural analysis of the CI complex by Hanafusa et al. [30] revealed that the chitosan chain in the CI crystal assumes a new type of 4/1 helical conformation alternative to the 2/1 or 8/5 helical types. With reference to the biological activities of the chitosan-iodine (CI) complex, Sashiwa et al. [31] showed that partially deacetylated chitin-isodine suspension has antimicrobial and wound healing activities.

From the objective of more effective utilization of chitosan and iodine as natural resources and the development of their novel functions, we have investigated the physicochemical properties, in particular, the coloring mechanism and structure of the CI complexes in solution [32, 33], in comparison with the amylose-iodine (AI) complexes. Our results can be summarized as follows: (a) When chitosan powder was directly dissolved in KI-I_2 solution containing acid (HNO_3, acetate buffer, etc.) at room temperature, the complexation was recognized by specific coloring. (b) However, when chitosan solution containing acid was mixed with KI-I_2 solution at room temperature, the complexation did not occur. (c) The color of the complex solution in (a) vanished when the temperature was raised to ca. 80°C, but restoration of the color was not observed even if the temperature was then lowered to 4°C. (d) When the uncomplexed (b) and (c) solutions were frozen, they developed the same color as the (a) solution. These observations indicated that thermal hysteresis, i.e., an irreversible reaction process, is involved in complexation and color formation. However, there is still no clear picture regarding the relationship between the thermal hysteresis phenomenon and the molecular characteristics, in particular, the solution structure of the CI complexes.

The present study was performed to analyze the spectroscopic properties of the CI complexes and to characterize the solution structures of chitosan and the CI complexes by various physicochemical techniques including circular dichroism (CD), resonance Raman spectroscopy, small-angle X-ray/neutron scattering (SAXS/SANS) measurements, and molecular dynamics (MD) calculations. We will also discuss the factors responsible for CI complexation and the thermal hysteresis behavior.

2. EXPERIMENTAL

2.1. Materials

Chitosan (C-9) from the queen crab shell was supplied by Kurita Water Industries, Ltd., and used without further purification. Its weight-average molecular weight (M_w) and molecular weight distribution (M_w/M_n) were $M_w = 1.1 \times 10^4$ and $M_w/M_n = 2.2$, respectively, as determined by size-exclusion chromatography coupled to a multiple-angle laser light-scattering (SEC-MALLS) using a DAWN-E model system (Wyatt Tech.). The DDA value of chitosan was 98% as determined by colloidal titration [34].

2.2. Preparation of CI Complexes

The CI complexes were prepared by freezing mixtures of chitosan and KI-I_2 solutions in the freezer compartment (ca. $-20°C$) of a refrigerator and then thawing them at 4°C. CI complex solutions were prepared over a wide concentration range of chitosan from 5×10^{-3} to 0.2 uM (u refers to one β-D-glucosamine unit) and I_2 5×10^{-4} to 3.5×10^{-3} M under the conditions of $[KI]/[I_2] = 10$. The main solvent used in this study was aqueous acetate buffer (0.33 M AcOH + 0.10 M NaOAc, pH 4.1). For SANS measurements with the contrast variation method [35], deuterated acetate buffer in heavy water D_2O was used, and the CI complex solutions were prepared using the mixed solvents of D_2O/(the D-buffer) and H_2O/(the H-buffer) with different D_2O contents (ϕ_D). The other acidic solvent for resonance Raman and ^{13}C-NMR measurements was aq 0.13 M HNO_3.

For preparation of thermally treated CI complex solutions, the samples were heated in sealed tubes to a given temperature and allowed to stand at this temperature for 10 min, then cooled to room temperature. This method was based on irreversibility of the CI complexation, and the treated samples were confirmed to be of the same color as those *in situ* at a given temperature.

2.3. Measurements

Absorption and CD spectra of the complexed solutions were obtained using a Shimazu UV-2101PC spectrophotometer and a Jasco J-725 spectropolarimeter, respectively, in which a thermostated cell controller is equipped. The light path length of the cell was 1 mm for both absorption and CD measurements. Raman spectra were measured with a Jasco NR-1000 spectrophotometer using an Ar^+ ion (514.5 and 488.0 nm) laser for excitation

with a rotary cell. ^{13}C-NMR measurements were performed on a JEOL JNM-EX400 NMR spectrometer.

Apparent sedimentation coefficients ($S^{app}_{20,w}$) and molecular weights (M^{app}) of the CI complexes and intact chitosan were determined at 20°C by the sedimentation velocity method and the sedimentation equilibrium method [36] using an Hitachi CP100a ultracentrifuge with an attached ABS-8 analytical UV monitor with the Hitachi software program. In the measurements, 12-mm double sector Epon resin cell centerpieces were used. M^{app} values were estimated from the Lamm equation:

$$M^{app} = \frac{2RT}{(1 - V\rho)\,\omega^2} \times \frac{d(\ln A)}{d(r^2)} \tag{1}$$

where A = absorbance at a given wavelength, which is proportional to the solute concentration and is measured with absorption optics; r = distance from the center of rotation; V = partial specific volume of the solute; ρ = density of the solvent; ω = angular velocity of the rotor; R = gas constant; and T = absolute temperature. In this study, V was taken to be 0.6 for all samples, referring to the average value of general polysaccharides [37].

SAXS measurements were performed at 25°C in the range of the scattering vector q ($=4\pi \sin(\theta/2)/\lambda$) of 6×10^{-3} to 0.2 Å^{-1} using a SAXS spectrometer installed at the BL-10C port in the Photon Factory of the National Laboratory for High Energy Accelerator Research Organization (Tsukuba, Japan). Sample-to-detector distance and wavelength λ were 188 cm and 1.49 Å, respectively. Structural analysis based on the total scattering curve was carried out by calculating the distance distribution function, $p(r)$, given by Fourier inversion of the scattering intensity $I(q)$ as

$$p(r) = \frac{2}{\pi} \int_0^\infty rqI(q) \sin(rq)\, dq \tag{2}$$

The radius of gyration, Rg, was then estimated by the equation [38]:

$$Rg^2 = \frac{\int_0^{D_{max}} p(r)\, r^2\, dr}{2 \int_0^{D_{max}} p(r)\, dr} \tag{3}$$

where D_{max} is the maximum dimension of the particle estimated from the condition $p(r) = 0$ for $r > D_{max}$.

SANS measurements with the contrast variation method [24, 35] were carried out at 20°C using a SANS spectrometer (SANS-U) installed at the C1-2 port of the cold-neutron beam line in the research reactor JRR-3M of the Japan Atomic Energy Research Institute (JAERI), Tokai, Japan.

The wavelength used was 7.0 Å and the sample-to-detector distances were 4 m (8×10^{-3} Å$^{-1} \leq q \leq 7 \times 10^{-2}$ Å^{-1}) and 1 m (4×10^{-2} Å$^{-1} \leq q \leq 0.25$ Å^{-1}). Structural analyses were performed based on the Stuhrmann plot from the SANS data. This procedure was described in detail elsewhere [24, 35].

2.4. MD Calculations

Prediction of the changes in the solution conformation of chitosan in the annealing process was carried out by the 500 ps MD calculation using the Discover module (CVFF as force field) of INSIGHT II from Molecular Simulation, Inc., under the conditions of distance-dependent dielectric constants ($\varepsilon = 1.8r$) with no cutoff for all interactions according to the following procedures [33, 39]: (a) The relaxed potential energy map of chitobiose (chitosan dimer) was determined based on the CVFF force field by optimizing the structures on a 10° grid spacing of the torsional angles about the glycosidic bonds (ϕ, ψ), referring to *the Cambridge Structural Database* for the initial structure. (b) The molecular models as starting samples for the MD calculation were constructed for chitosans with degrees of polymerization (DP) of 20, 30, and 50 based on the dimer structure of the energy minimum. (c) MD calculations for the heating process were carried out at 298 K and then at 1200 K, where a number of conformations were generated. (d) MD calculations in the cooling process from 1200 K were done stepwise at 500 K and then at 298 K for each of several 1200 K-generated conformations selected randomly as starting samples. The conformations at 298 K were confirmed to become stable with small energy fluctuation around the equilibrium state at the final stage in the 500 ps calculation. (e) For comparison, the same MD calculation was carried out for amylose chains.

3. RESULTS AND DISCUSSION

3.1. Spectroscopic Properties

Figures 1a and b show typical absorption and CD spectra of the purple-colored CI complex at about 25°C, including the I_2 concentration dependences of the absorbance (A_{500}) and ellipticities ($\theta_{460}, \theta_{540}$) at the maximum wavelengths at a given concentration of chitosan. As a reference, the absorption spectrum for free I_2/KI solution is also shown. The complex exhibited an absorption spectrum with a peak at 500 nm, and mutually split CD bands with opposite signs (+, −). It should be noted that these spectral characteristics were independent of the concentrations of iodine

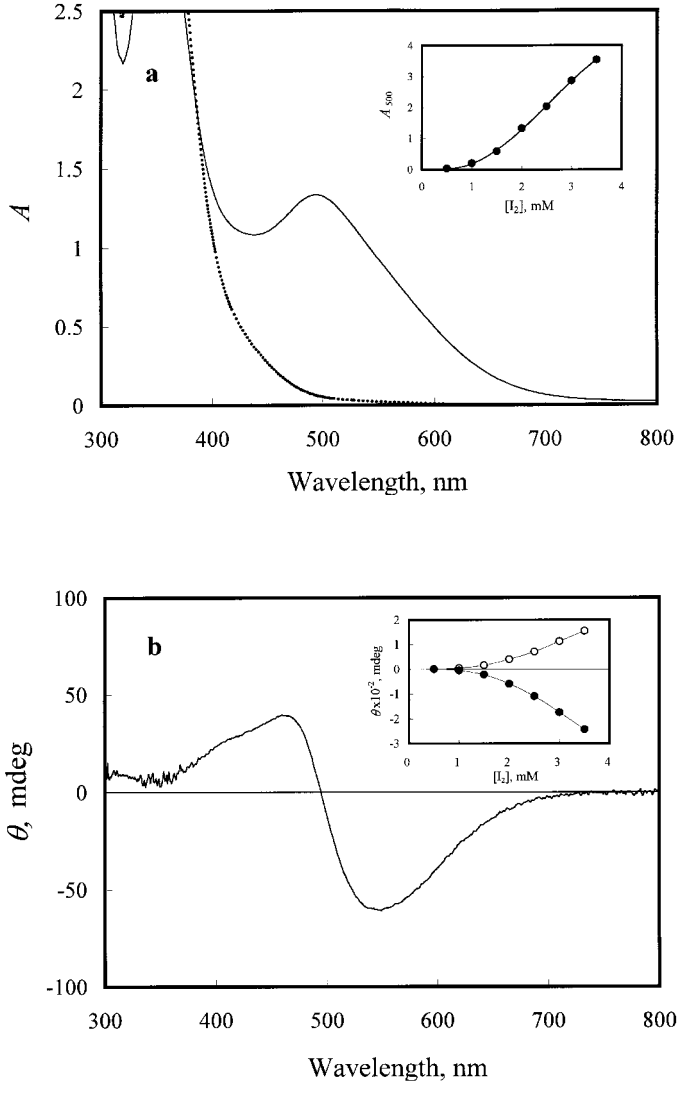

Fig. 1. Absorption (a) and CD (b) spectra of the CI complex in 0.33 M acetate buffer, including the absorption spectrum of free I_2-KI solution (dotted line). Conc.: $[\text{chitosan}] = 2 \times 10^{-2}$ uM; $[I_2] = 2 \times 10^{-3}$ M; $[KI] = 2 \times 10^{-2}$ M. Inset: (a) Absorption (A_{500}) at 500 nm and (b) ellipticities (θ_{460} ○, θ_{540} ●) at 460 and 540 nm as a function of I_2 concentration, where the maximum wavelengths (a, 500 nm; b, 460 nm, 540 nm) of the absorption and CD bands for the CI complex remained unchanged *versus* the change in I_2 concentration. The light path length of the cell was 1 mm for both absorption and CD measurements.

and chitosan, temperature and acid species [32] and were similar to those of AI complexes [20]. We have concluded that the coloring of AI complexes was developed by the left-handed *iodine/iodide dimer exciton-coupled mechanism* involving *charge-transfer* between iodine/iodide and the amylose chain and the *configuration interaction* among the electronic transition states of iodine/iodide [20, 22]. The coloration of the CI complexes could be interpreted in terms of a similar mechanism.

A sharp increase in the A_{500} value with I_2 concentration appeared at a threshold I_2 concentration ($[I_2]/[\text{chitosan}] \approx 0.05$) at a given chitosan concentration (0.02 uM) in accordance with the increase in θ_{460} and θ_{540}, up to a high concentration (3.5×10^{-3} M), above which precipitation of the CI complexes was observed. Similar cooperative behavior for iodine incorporation in chitosan was observed regardless of the chitosan concentration. On the other hand, as for the effect of chitosan concentration, the A_{500} values tended to monotonically increase with chitosan concentration at a given I_2 concentration in accordance with the increase in θ_{460} and θ_{540} up to a high concentration ($[I_2]/[\text{chitosan}] \approx 0.1$) and then level off or gradually decrease [40]. Therein, the maximum wavelengths of the absorption and CD bands for the CI complex remained unchanged *versus* the change in chitosan concentration in the same way as with the change in I_2 concentration. Similar behavior for the effect of chitosan concentration was observed regardless of the iodine concentration. It should be noted that, regarding the aging after complex preparation, the CI complex was appreciably stable on storage at a low temperature of 4°C even over a long incubation period of about 6 months. However, it was unstable at room temperature and the purple color of the CI complex solution was apt to fade with aging time, the extent of which depended on iodine and chitosan concentrations. This behavior would be ascribed to hydrolysis of I_2, in which the action of the basic glucosamine resides is involved.

The effects of temperature on the optical quantities in the heating and cooling processes are shown for A_{500} and θ_{460} or θ_{540}, respectively, in Fig. 2a and b. In the heating process, both of the optical quantities decreased sharply above 30°C and then the color completely disappeared at ca. 60°C. Therein, the maximum wavelengths of the absorption and CD bands for the CI complex remained unchanged *versus* the change in temperature. On the other hand, in the cooling process after the disappearance of the color, neither of the optical quantities was restored even if the temperature was lowered to 4°C. However, when the solution was frozen and then thawed, the optical quantities showed complete restoration. These results indicated that the CI complexation is essentially irreversible, in contrast to AI complexation [41]. We confirmed that the restoration of this thermal hysteresis behavior could be repeated at least five times. However, an exact

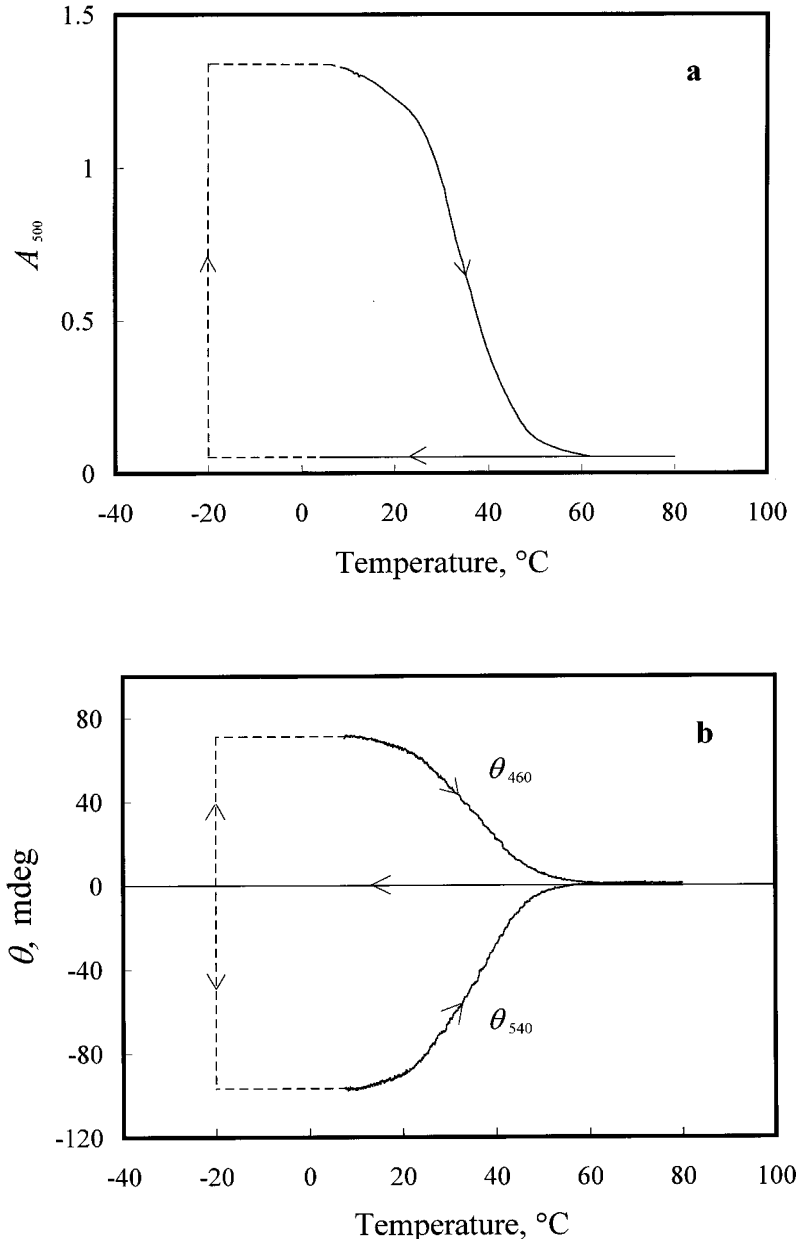

Fig. 2. (a) A_{500} and (b) θ_{460} and θ_{540} as a function of temperature. Heating and cooling rates were $2°C \cdot min^{-1}$. The broken lines refer to the unmeasured and predicted values.

interpretation of the mechanism of the coloring restoration induced by freezing of the chitosan-iodine mixed solution has not yet been established. Furthermore, useful information on the stoichiometric and kinetic properties for the CI complexation has not yet been obtained.

The resonance Raman spectra of the CI complex in aq HNO_3 are shown in Fig. 3 with respect to the 488.0- and 514.5-nm excitations. The Raman spectrum of free I_2-KI solution is included as a reference. Raman spectra exhibited strong scattering at 110 cm^{-1} and weaker scattering at 150 cm^{-1} as fundamental tones regardless of the excitation wavelength. In addition, an overtone band at 110 cm^{-1} appeared at 220 cm^{-1}. Similar spectral characteristics were obtained in the other acid-species systems. The

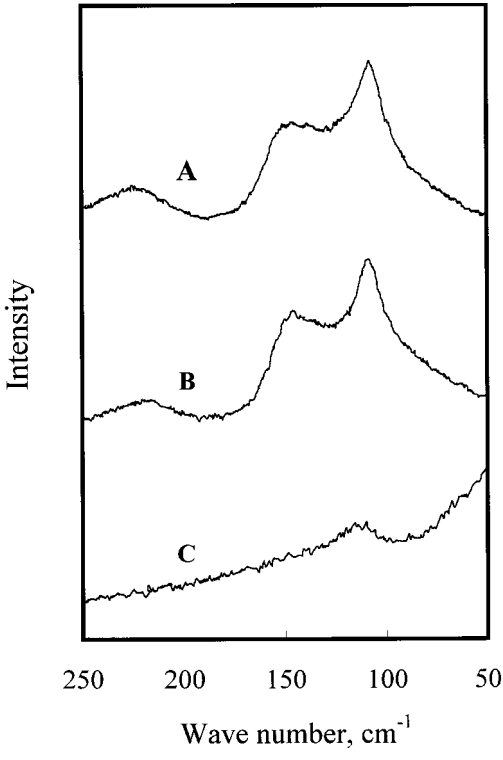

Fig. 3. Resonance Raman spectra of the CI complex in aq 0.13 M HNO_3 excited at 488.0 nm (A) and 514.5 nm (B). The Raman spectrum of free I_2-KI solution excited at 514.5 nm (C) is included as a reference. Conc.: $[\text{chitosan}] = 5 \times 10^{-2}$ uM; $[I_2] = 1 \times 10^{-3}$ M; $[KI] = 1 \times 10^{-2}$ M.

other iodine/iodide complexes of amylose [42] and poly(vinyl alcohol) [43] also had similar fundamental Raman lines (160 and 110 cm^{-1}), although the 160-cm^{-1} lines in their Raman spectra were stronger than the 110-cm^{-1} lines. The 110-cm^{-1} lines of the CI complex and free iodine/iodide were assigned to the I_3^- symmetric stretching vibration, whereas the 150-cm^{-1} line was assigned to the I_5^- asymmetric stretching vibration [42–44]. Therefore, it was concluded that the bound iodine species responsible for the coloring of CI complexes is primarily I_3^- ions.

To obtain information regarding the iodine-binding sites of glucosamine residues, the changes in the chemical shifts in the ^{13}C-NMR spectra of chitosan induced by CI complexation were examined. The ^{13}C-NMR spectrum of the CI complex in aq HNO_3 measured using MeOH as an external reference is shown in Fig. 4, where the assignment of each of the signal peaks is given in the figure [16]. The effect of the iodine-binding on the chemical shift of each peak is summarized in Table I. Only C-1, C-3, and C-4 signals are shifted to a higher field due to the effect of heavy atoms such as iodine on the nuclear shielding constant [45]. Similar results were obtained in the other acid-species systems in the same way as for the other spectral characteristics. Therefore, the interaction sites in the glucosamine residues in chitosan with bound iodine were inferred to be the OH groups or glycosidic oxygen atoms on C-1, C-3, and C-4; the amino group for C-2

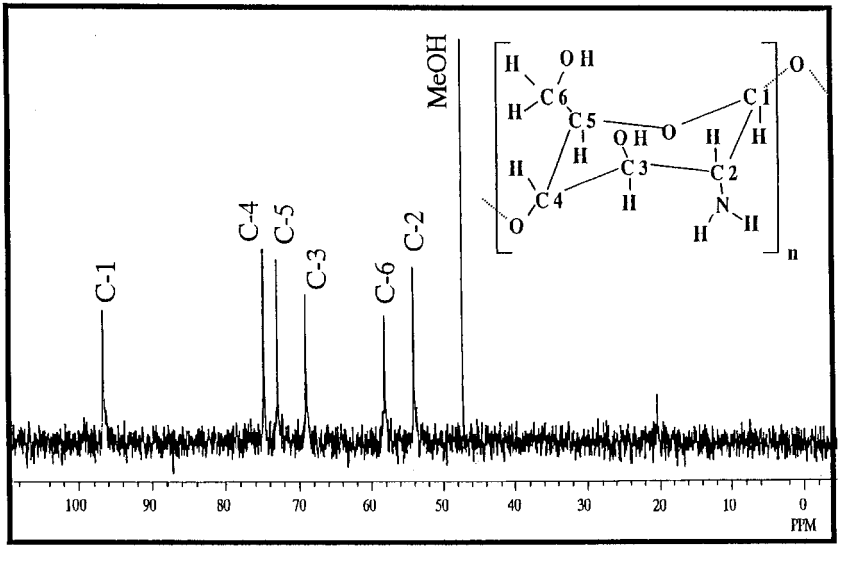

Fig. 4. ^{13}C-NMR spectrum of the CI complex in aq 0.13 M HNO_3 using MeOH as an external standard. Conc.: [chitosan] = 0.184 uM; $[I_2] = 5 \times 10^{-3}$ M; $[KI] = 5 \times 10^{-2}$ M.

Table I. Effects of the CI Complexation on the Chemical Shifts of the ^{13}C-NMR Signals of the β-D-glucosamine Residues in Chitosan

Carbon	Chitosan, ppm	CI complex, ppm	Dd, ppm
C-2	53.8	53.8	0.0
C-6	58.0	58.0	0.0
C-3	68.3	68.1	−0.2
C-5	72.8	72.8	0.0
C-4	74.4	74.3	−0.1
C-1	95.8	95.6	−0.2

was not responsible for the binding of iodine. The latter would deny the concept of Shigeno et al. [28, 29] that iodine binding is caused by the formation of charge-transfer complexes between the amino groups of chitosan and iodine. Moreover, the latter is supported by the findings that cellulose, a linear polysaccharide of β-(1, 4) linked D-glucoses, formed a colored complex with iodine in excess aqueous $ZnCl_2$ in the same way as with amylose [46].

3.2. Structural Studies

Apparent molecular weights (M^{app}) of the CI complexes, estimated from Eq. (1) by sedimentation equilibrium measurements under conditions of $[I_2]/[\text{chitosan}] = 0.1$, are summarized as a function of treatment temperature in Fig. 5. It should be noted that the treated samples were confirmed to possess the same coloring abilities as those *in situ* at each temperature from the irreversibility of the complexation, as described in Section 2.2. Surprisingly, the M^{app} value at 20°C was 3.8×10^5 ($S^{app}_{20,w} = 13.0$ S), about 35-fold higher than that of intact chitosan ($M^{app} = 1.1 \times 10^4$, $S^{app}_{20,w} = 0.4$ S), which coincided with the M_w value determined from the SEC-MALLS measurement. The M^{app} value decreased markedly above 30°C with temperature, following the coloring decline, and approached the M^{app} value of intact chitosan. In view of the observation that the relative number of glucosamine residues to one I_2 molecule was 10 in this experiment, this result implies that the molecular assembly of chitosan through the interaction with iodine plays a vital role in the colored CI complexation associated with the effect of iodine and/or chitosan concentrations on complexation.

Subsequently, the characterization of aggregate structures of the CI complexes was carried out based on analyses of the SAXS data. Figure 6 shows the measured SAXS curves of chitosan and the CI complex at 25°C, where the signal-to-noise ratio for chitosan is small because of the weak

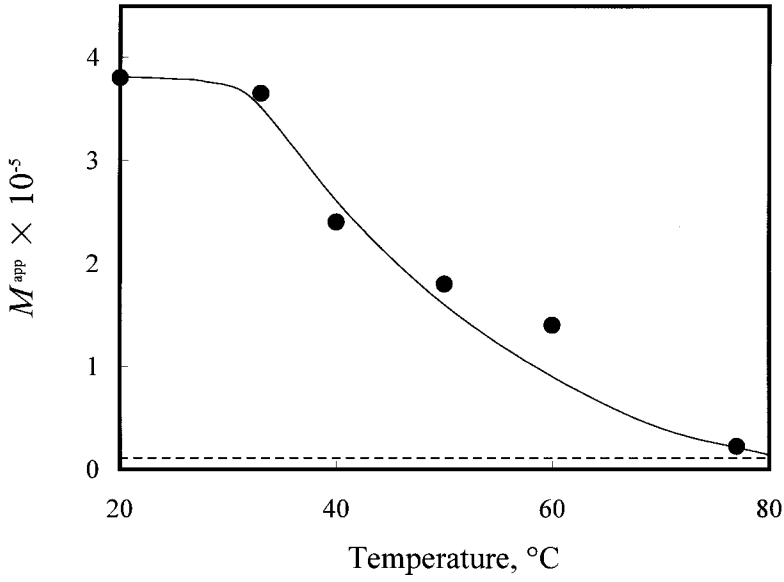

Fig. 5. Apparent molecular weight (M^{app}) of the CI complex as a function of treatment temperature in 0.33 M acetate buffer. The broken line refers to the M^{app} value of chitosan. Conc.: $[\text{chitosan}] = 2 \times 10^{-2}$ uM; $[I_2] = 2 \times 10^{-3}$ M; $[KI] = 2 \times 10^{-2}$ M. The measurements for the CI complexes were carried out at a wavelength in the range of 480 nm to 660 nm corresponding to $A \approx 0.6$ with the light path length of 1 cm, whereas for chitosan, the wavelength was fixed at 235 nm.

$I(q)$, including the distance distribution functions, $p(r)$ (Eq. (2)). The Rg values estimated by Eq. (3) from the resulting $p(r)$ functions were 27.3 Å ($D_{max} = 55$ Å) for chitosan and 78.2 Å ($D_{max} = 190$ Å) for the CI complex, which corresponded to a significant increase in the M^{app} value following the complexation. From the viewpoint of the resulting $p(r)$ shapes, simulation of the $p(r)$ curves of chitosan and the CI complex was carried out with the theoretical scattering functions for an ellipsoid and a cylinder composed of two layers [47], respectively. As a result of fitting to the Rg values as well as the $p(r)$ curves, the solution structure of chitosan was characterized by an ellipsoid with a major semiaxis of 30 Å and minor semiaxis of 10 Å, whereas the aggregate structure of the CI complex was characterized by a two-layer cylinder with a height of 210 Å, an inner radius of 10 Å, and an outer radius of 20 Å, assuming that the inner scattering density was about two-fold larger than the outer density. The resulting $I(q)$ and $p(r)$ functions corresponding to each of the theoretical models are shown by the solid lines in Fig. 6. Taking into account the virtual bond length of 5.5 Å between the glucosamine residues and the average DP

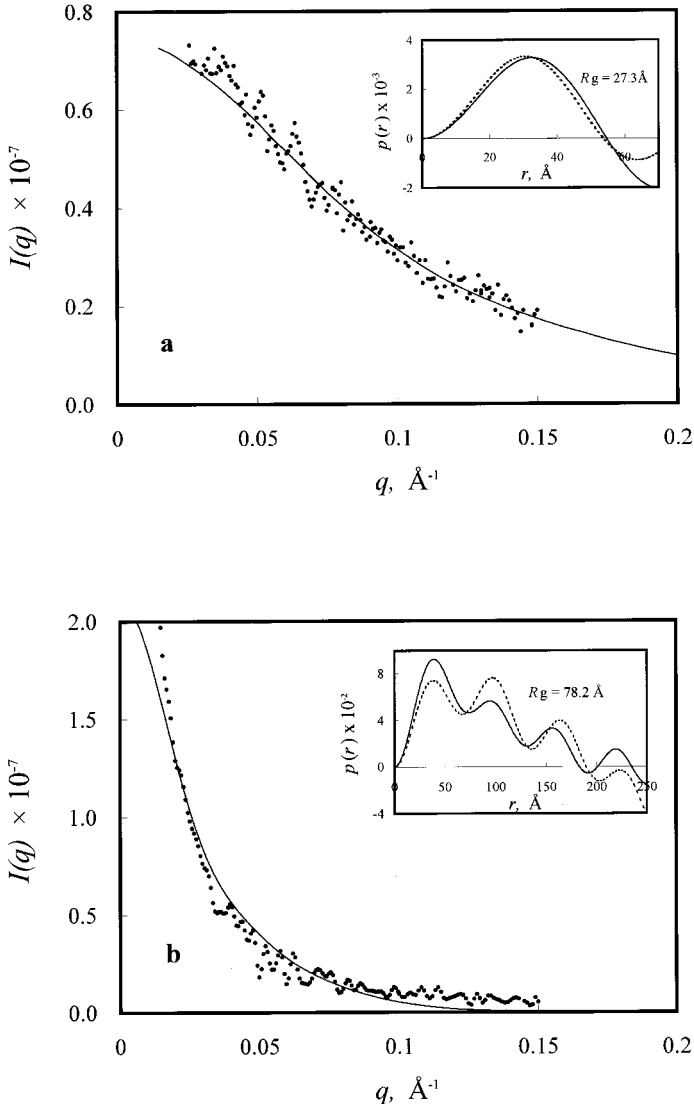

Fig. 6. Measured SAXS curves of chitosan (a) and the CI complex (b) in 0.33 M acetate buffer. The inset shows the $p(r)$ functions. Conc.: [chitosan] $= 2 \times 10^{-2}$ uM; $[I_2] = 2 \times 10^{-3}$ M; $[KI] = 2 \times 10^{-2}$ M. The solid lines refer to the theoretical $I(q)$ and $p(r)$ functions: (a) ellipsoidal model with a major semiaxis of 30 Å and minor semiaxis of 10 Å; (b) two-layer cylindrical model with a height of 210 Å, an inner radius of 10 Å, and an outer radius of 20 Å, assuming that the inner scattering density was about two-fold larger than the outer density.

(ca. 70) of chitosan used in this study, it is assumed that free chitosan undergoes a compactly folded conformation involving intramolecular hydrogen bonds, whereas the chitosan chains in the CI aggregate assume a crystalline-like extended conformation [5–8, 10, 30]. The two-layer cylindrical model for the aggregate structure of the CI complex was supported by the results of structural analysis of the SANS data based on the Stuhrmann plot [35, 47], in which the *R*g value at infinite contrast (*R*g, c), the radial second moment of the mean scattering length density (SD), α, and the derivation of the center of the SD distribution with respect to the center of the geometrical shape, β, were estimated to be *R*g, c = 91.6 Å, $\alpha = -74.2$, and $\beta = 0$ Å^{-2}. For intact chitosan, these values were *R*g, c = 40.4 Å, $\alpha = -10.0$, and $\beta = 29.6 \times 10^{-10}$ Å^{-2}. Further details of the SANS studies were be reported elsewhere [48]. SAXS and SANS structural analyses suggested that the CI complex forms an aggregate with a two-layer cylindrical structure composed of an inner polyiodide chain surrounded by an assembly of crystalline-like extended chitosan chains involving an intermolecular hydrogen bond network composed of N2 $\cdots$ O6 hydrogen bonds and water bridges [8, 10]. This structural characteristic of the CI complex would be analogous to that proposed for the poly(vinyl alcohol)-iodine complex [23, 24] but differs from that of the AI complex in which iodine/iodide molecules are included in six-fold, left-handed helical V-amylose [49]. From structural X-ray diffraction studies, it has been revealed that the chitosan chain in the CI crystal assumes a 4/1 helical conformation [30]. One of our findings, (a) described in Section 1, could be interpreted in terms of the requirement of the crystalline-like extended chitosan chains for coloring of the complex.

Figure 7 shows the effects of treatment temperature on the *R*g values estimated by Eq. (3) from the resulting $p(r)$ functions. The *R*g value tended to decrease with temperature above 30°C, corresponding to the M^{app} behavior (see Fig. 5), accompanying a decline in color. The above results including the $p(r)$ functions suggested that the aggregate structure of the CI complex starts to be destroyed at ca. 30°C, followed by dissociation of the intermolecular hydrogen bond network of chitosan chains and the release of bound iodine/iodide, and that the complex is transformed with temperature from a cylindrical structure to a compacted ellipsoid or spherical structure of free chitosan chains.

3.3. MD Calculations

To determine the factors involved in the irreversibility of CI complexation, the solution conformations of chitosan chains were predicted according to the procedures described in Section 2.4, in comparison with that for amylose chains. The current lowest energy conformation of a long chitosan

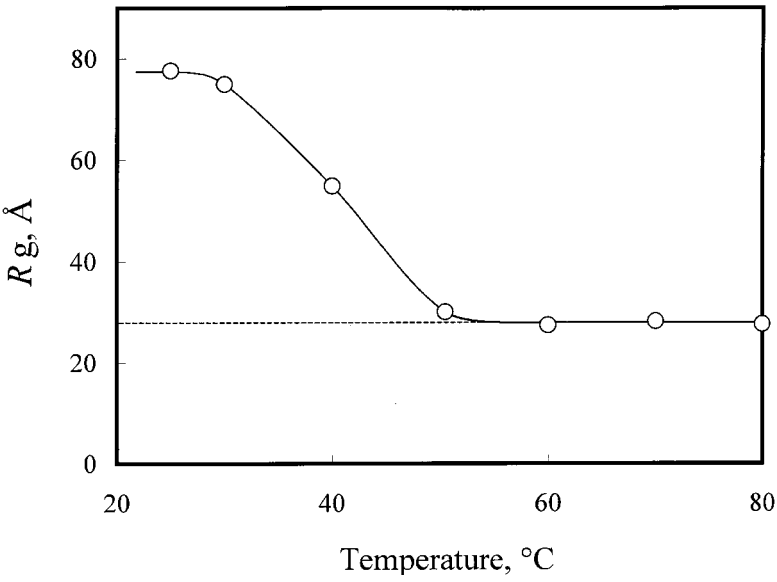

Fig. 7. *R*g estimated by Eq. (3) from the resulting $p(r)$ function as a function of treatment temperature. The broken line refers to the *R*g value of chitosan.

chain was predicted to be an extended conformation similar to the crystalline conformation [8, 10] based on the torsion angles ($\phi = 45.7°$, $\psi = -14.4°$) for the energy minimum in the counter map of chitobiose, whereas the current lowest energy conformation of the amylose chain was predicted to be a 6/1 helical structure similar to the crystalline conformation [49] from the torsion angles ($\phi = -11.6°$, $\psi = -18.2°$) for the maltose energy minimum. The pyranose rings in both the chitosan and amylose chains with the current lowest energy conformations assumed the standard $^4C_1$ chair conformation. MD simulations for the chitosan and amylose chains in the heating (298 → 1200 K) and cooling (1200 → 298 K) processes were carried out using the predicted extended and 6/1 helical structures, respectively, as starting samples. The MD simulations showed that the extended conformation of chitosan tends to be transformed into a folded conformation like an antiparallel β-sheet of protein upon the dissolution in solution or with increasing temperature, associated with the conformational changes in pyranose rings that are a part of the β-D-glucosamine residues and the formation of intramolecular hydrogen bonds in chitosan. However, the folded conformation could not be easily restored to the extended form by decreasing the temperature, owing to the effect of long-range intramolecular hydrogen bonding. In contrast, the final conformation

of the amylose chain fluctuated around the original helical structure and could be restored by cooling. Further details of the MD simulation will be reported elsewhere. The β-sheet-like folded conformations of chitosan are located close to the lowest energy extended conformation, but the distribution of states is highly rugged and this would result in a long half-life of the trapped states at one of the folded conformations, as suggested by the random energy model [50]. These conformational properties of chitosan are likely to be responsible for the irreversibility of CI complexation. It should be noted that the theoretical scattering function and the $p(r)$ function for the compactly folded conformations were in good agreement with the experimental results. Further probed studies would be required to rationalize the mechanism of the conformational transition of chitosan from the compactly folded form to the crystalline-like extended form during the restoration of the CI complexation induced by freezing.

4. CONCLUSIONS

The results of the present study indicated that a stable conformation of chitosan in solution would be a folded structure, that it does not form a colored complex with iodine, and that the irreversibility and thermal hysteresis behavior as unique characteristics of the CI complexes would be governed by a crystalline-like extended $\rightarrow$ compactly folded conformational transition of chitosan in solution. Moreover, it was found that a cylindrically-shaped assembly of extended chitosan chains including iodine/iodide molecules is significantly involved in the colored CI complexation.

ACKNOWLEDGMENTS

This work was supported in part by a Grant-in-Aid for Scientific Research No. 12650889 from the Ministry of Education, Science, Sports, and Culture of Japan. We are greatly indebted to Mr. N. Kawashima, Mr. Y. Suzuki, Mr. T. Sakajiri, and Mr. H. Tanaka of the Science University of Tokyo for their technical assistance.

REFERENCES

1. P. A. Sandford, in *Chitin/Chitosan*: *Sources*, *Chemistry*, *Biochemistry*, *Physical Properties*, *and Applications*, G. Skjak-Braek, T. Anthonsen, and P. A. Sandford, eds. (Elsevier, Amsterdam, 1990), p. 51.
2. P. A. Sandford and G. P. Hutchings, in *Industrial Polysaccharides*, M. Yalpani, ed. (Elsevier, Amsterdam, 1987), p. 363.
3. W. Malette, M. Quigley, and E. Adicks, in *Chitin in Nature and Technology*, R. Muzzarelli, C. Jeuniaux, and G. Gooday, eds. (Plenum Press, New York, 1986), p. 435.

4. S. Minami, Y. Okamoto, A. Matsuhashi, H. Sashiwa, H. Saimoto, Y. Shigemasa, T. Tanigawa, Y. Tanaka, and S. Tokura, in *Advances in Chitin and Chitosan*, C. J. Brine, P. A. Sandford, and J. P. Zikakis, eds. (Elsevier Applied Science, London, 1992), p. 61.
5. K. Ogawa and S. Inukai, *Carbohydr. Res.* **160**:425 (1987).
6. T. Yui, K. Imada, K. Okuyama, Y. Obata, K. Suzuki, and K. Ogawa, *Macromolecules* **27**:7601 (1994).
7. K. Mazeau, W. T. Winter, and H. Chanzy, *Macromolecules* **27**:7606 (1994).
8. K. Okuyama, K. Noguchi, M. Kanenari, T. Egawa, K. Osawa, and K. Ogawa, *Carbohydr. Polym.* **41**:237 (2000).
9. H. Saito, R. Tabeta, and K. Ogawa, *Macromolecules* **20**:2424 (1987).
10. K. Okuyama, K. Noguchi, T. Miyazawa, T. Yui, and K. Ogawa, *Macromolecules* **30**:5849 (1997).
11. M. Terbojevich, A. Cosani, B. Focher, A. Naggi, and G. Torri, *Carbohydr. Polym.* **18**:35 (1992).
12. M. W. Anthonsen, K. M. Vårum, and O. Smidsrød, *Carbohydr. Polym.* **22**:193 (1993).
13. N. Errington, S. E. Harding, K. M. Vårum, and L. Illum, *Int. J. Bio. Macromol.* **15**:113 (1993).
14. M. L. Tsaih and R. H. Chen, *Int. J. Bio. Macromol.* **20**:233 (1997).
15. R. G. Beri, J. Walker, E. T. Reese, and J. E. Rollings, *Carbohydr. Res.* **238**:11 (1993).
16. A. Domard, C. Gey, M. Rinaudo, and C. Terrassin, *Int. J. Biol. Macromol.* **9**:233 (1987).
17. T. Yui, H. Kobayashi, S. Kitamura, and K. Imada, *Biopolymers* **34**:203 (1994).
18. C. Yomota, T. Miyazaki, and S. Okada, *Colloid. Polym. Sci.* **271**:76 (1993).
19. L. A. Berkovich, G. I. Timofeyeva, M. P. Tsyurupa, and V. A. Davankov, *Polym. Sci. USSR* **22**:2009 (1980).
20. T. Handa and H. Yajima, *Biopolymers* **18**:873 (1979).
21. T. Handa and H. Yajima, *Biopolymers* **20**:2051 (1981).
22. H. Yajima, T. Nishimura, T. Ishii, and T. Handa, *Carbohydr. Res.* **163**:11 (1987).
23. H. Takamiya, Y. Tanahashi, T. Matsuyama, T. Taniguchi, K. Yamaura, and S. Matsuzawa, *J. Appl. Polym. Sci.* **50**:1807 (1993).
24. H. Yajima, *J. Cryst. Soc. Jpn.* **36**:142 (1994).
25. F. L. Campbell, *Ann. Entomol. Soc. Am.* **22**:401 (1929).
26. B. D. E. Gaillard and R. W. Bailey, *Nature* **212**:202 (1966).
27. R. A. A. Muzzarelli, in *Chitin* (Pergamon, New York, 1977), p. 150.
28. Y. Shigeno, K. Kondo, and K. Takemoto, *J. Appl. Polym. Sci.* **25**:731 (1980).
29. Y. Shigeno, K. Kondo, and K. Takemoto, *Angew. Makromol. Chem.* **91**:55 (1980).
30. Y. Hanafusa, K. Osawa, K. Noguchi, K. Okuyama, and K. Ogawa, *Polym. Prepr. Jpn.* **48**:3853 (1999); **49**:404 (2000).
31. H. Sashiwa, Y. Okamoto, S. Minami, and Y. Shigemasa, *Chitin and Chitosan Res.* **4**:18 (1998).
32. T. Morita, Y. Tezuka, H. Yajima, and T. Ishii, *Polym. Prepr. Jpn.* **46**:382 (1997).
33. H. Yajima, Y. Suzuki, M. Kamoshita, K. Tsunoda, T. Ishii, and T. Kikuchi, *Polym. Prepr. Jpn.* **47**:3520 (1998).
34. H. Terayama, *J. Polym. Sci.* **8**:243 (1952).
35. H. Yajima, H. Yamamoto, M. Nagaoka, K. Nakazato, T. Ishii, and N. Niimura, *Biochim. Biophys. Acta* **1381**:68 (1998).
36. A. Tiselius, in *Methods in Enzymology*, Vol. 4, S. P. Colowick and N. O. Kaplan, eds. (Academic Press, New York, 1957), p. 35.
37. M. D. Lechner, E. Nordmeier, and D. G. Steinmeier, in *Polymer Handbook*, J. Brandrup, E. H. Immergut, and E. A. Grulke, eds. (John Wiley, New York, 1999), p. VII/85.

38. O. Glatter, in *Small Angle X-ray Scattering*, O. Glatter and O. Kratky, eds. (Academic Press, 1982), p. 119.
39. Y. Suzuki, H. Yajima, K. Tsunoda, T. Ishii, and T. Kikuchi, *Polym. Prepr. Jpn.* **48**:886 (1998).
40. M. Kamoshita, K. Tsunoda, H. Sashiwa, M. Hashimoto, M. Morita, H. Yajima, and T. Ishii, *Chem. Soc. Jpn. Nat. Meeting* **76**:763 (1999).
41. G. L. Hatch, *Anal. Chem.* **54**:2002 (1982).
42. T. Handa and H. Yajima, *Biopolymers* **19**:1723 (1980).
43. Y. Oishi, H. Yamamoto, and K. Miyasaka, *Polym. J.* **19**:1261 (1987).
44. H. Kim, *Biopolymers* **21**:2083 (1982).
45. I. Morishima, K. Endo, and T. Yonezawa, *J. Chem. Phys.* **59**:3356 (1973).
46. T. Abe, *Bull. Chem. Soc. Jpn.* **31**:661 (1958).
47. L. A. Feigin and D. I. Svergun, in *Structure Analysis by Small-Angle X-ray and Neutron Scattering* (Plenum, New York, 1987), p. 59.
48. H. Yajima, Y. Suzuki, T. Sakajiri, and T. Ishii, *Activity Report on Neutron Scattering Research* **7**:262 (2000).
49. D. French, in *Starch: Chemistry and Technology*, R. L. Whistler, J. N. Bemiller, and E. F. Paschall, eds. (Academic Press, San Diego, 1984), p. 183.
50. J. D. Bryngelson, J. N. Onuchic, N. D. Socci, and O. G. Wolynes, *Proteins* **21**:167 (1995).